Characterization of a potent antimicrobial lipopeptide via coarse-grained molecular dynamics ☆

Joshua N. Horn, Jesse D. Sengillo, Dejun Lin, Tod D. Romo, Alan Grossfield *

Department of Biochemistry and Biophysics, University of Rochester Medical Center, 601 Elmwood Ave, Box 712, Rochester, NY 14642, USA

ARTICLE INFO

ABSTRACT

The prevalence of antibiotic-resistant pathogens is a major medical concern, prompting increased interest in the development of novel antimicrobial compounds. One such set of naturally occurring compounds, known as antimicrobial peptides (AMPs), have broad-spectrum activity, but come with many limitations for clinical use. Recent work has resulted in a set of antimicrobial lipopeptides (AMLPs) with micromolar minimum inhibitory concentrations and excellent selectivity for bacterial membranes. To characterize a potent, synthetic lipopeptide, C16-KGG**K**, we used multi-microsecond coarse-grained simulations with the MARTINI forcefield, with a total simulation time of nearly 46 μs. These simulations show rapid binding of C16-KGG**K**, which forms micelles in solution, to model bacterial lipid bilayers. Furthermore, upon binding to the surface of the bilayer, these lipopeptides alter the local lipid organization by recruiting negatively charged POPG lipids to the site of binding. It is likely that this drastic reorganization of the bilayer has major effects on bilayer dynamics and cellular processes that depend on specific bilayer compositions. By contrast, the simulations revealed no association between the lipopeptides and model mammalian bilayers. These simulations provide biophysical insights into lipopeptide selectivity and suggest a possible mechanism for antimicrobial action. This article is part of a Special Issue entitled: Membrane protein structure and function.

1. Introduction

Antimicrobial peptides (AMPs) are naturally occurring compounds found in virtually all multicellular organisms, and serve as critical components of the innate immune system [1]. First isolated from insects in the early 1980s [2] and from tree-frogs in the late 1980s [3], these compounds were quickly noted for their potency against bacteria [4,5]. To date, over 1700 antimicrobial peptides have been cataloged from a variety of species [6,7]. These compounds tend to share a common set of characteristics, specifically a positive charge and an amphipathic structure [8].

AMPs have garnered increased interest over the last two decades as potential new drug candidates [9], as many inhibit bacterial growth at micromolar or even nanomolar concentrations [10]. This potential lies in the fact that AMPs are less likely to induce evolved resistance in their targets, as they permeabilize the lipid bilayer by targeting the specific composition of the bacterial membrane and directly affecting membrane lipids [11]. Their cationic nature provides selectivity to bacterial membranes, which are generally anionic due to large concentrations of negatively charged lipid species. Their amphipathic

structure allows for binding and interaction with the lipid bilayer. Beyond this general hypothesis, the specific mechanism of membrane perturbation is unknown. A number of models have been suggested, including pore formation [12], detergent-like permeabilization of the bilayer [13], and membrane destabilization after AMPs coat the bilayer surface [14]. Moreover, it seems likely that there is no single mechanism to explain AMP action; rather, different AMPs may be described by one or more of the above models.

Despite the optimism, most AMPs are not ideal drug candidates. Because of their size, they tend to be prohibitively expensive to produce in quantities large enough to be effective. Also, bioavailability is a concern, as peptidases would degrade free peptides in the body [15]. With this in mind, the Shai group examined the effects of lipidating small peptides to construct easily-synthesized molecules with the same basic properties of AMPs. They demonstrated that conjugating fatty acids to short peptides that were in themselves membrane-inert could bestow membrane-active antimicrobial properties [16,17]. In fairly recent work, the Shai lab developed a set of antimicrobial lipopeptides (AMLPs) with broad-spectrum antibacterial and antifungal activity. They have a common architecture, including a fatty acid chain conjugated to a 4-residue peptide, of which 2 are lysines, yielding a net +2 charge. These molecules also include 1 D-amino acid to prevent peptidase activity (D-enantiomer denoted with bold lettering) [18]. The most potent of these molecules, C16-KGG**K** (where C16 indicates a 16-carbon saturated fatty acid chain attached to the N-terminus), has a minimum inhibitory concentration (MIC) in the micromolar range for

common strains of various pathogens. Further work showed C16-KGG**K** has a similar MIC against plant-pathogenic bacteria [19].

Probing the mechanism of action behind these specific AMLPs provides an approachable problem for molecular dynamics simulation. Great strides have already been made using MD to address problems in membrane biophysics [20–22], including antimicrobial peptides [23]. For many AMPs, sampling conformational space can prove challenging, especially if they are relatively unstructured in solution. C16-KGG**K**, however, is small, making conformational sampling computationally tractable. The limiting factor then becomes sampling the slow-timescale adjustments of the bilayer due to the presence of the lipopeptides.

To address this issue, coarse-graining (CG) approaches are frequently employed. In this kind of model, individual atoms are merged into larger particles that retain the underlying properties of the abstracted atoms. This dramatically reduces computational cost by reducing the number of degrees of freedom in the system, allowing for the use of significantly larger time steps for the integration of the equations of motion. Recent work has shown success in simulating AMPs using the MARTINI coarse-grained force field, which boasts speeds two orders of magnitude greater than conventional all-atom models [24,25]. This allows investigators to simulate many more systems, as well as larger systems, than are usually feasible in these kinds of studies.

In this study, we explore the selectivity and mechanism of activity of C16-KGG**K** using coarse-grained molecular dynamics simulation. Multiple multi-microsecond simulations employing the MARTINI force field were performed with two systems designed to serve as model replicas of "bacteria-like" and "mammal-like" bilayers. We demonstrate selectivity of C16-KGG**K** for bacterial bilayers and hypothesize that the effect is electrostatically driven. Further analysis of the bacterial systems shows some striking bilayer effects and implies a possible mechanism for the antibacterial activity of this AMLP.

2. Methods

2.1. System construction

The MARTINI coarse-grained force field was used to model our system of interest [26,27]. Construction of C16-KGG**K** was done by merging the MARTINI models for lipid tails and peptides. Initial configurations for CG C16-KGG**K** were constructed by overlaying the CG model on an all-atom representation (see Fig. 1). To model the peptide's innate flexibility, no secondary structure restraints were applied.
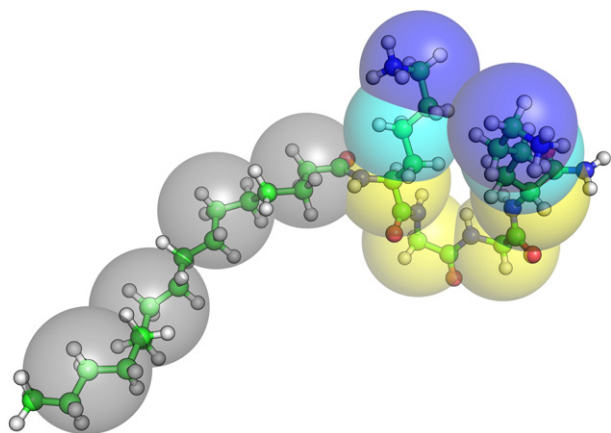
Fig. 1. Coarse-grained representation of the lipopeptide C16-KGG**K** (MARTINI model) overlaying a ball-and-stick all-atom representation. The non-polar saturated fatty acid tail is represented by gray spheres. Individual peptide backbone segments are represented by yellow spheres, apolar lysine chains by turquoise, and each lysine's charged sidechain amino group by blue.

We simulated two unique membrane systems. The first represents a "gram-negative bacteria-like" bilayer, with a 2:1 phosphatidylethanol-amine (POPE):phosphatidylglycerol (POPG) bilayer. This simplified representation and specific composition was chosen for its similarity to model membranes commonly used in experiment. The second was a "mammal-like" bilayer, with pure phosphatidylcholine (POPC). Each system totaled 480 lipids, split and distributed evenly between the two leaflets. The 2:1 ratio of POPE:POPG was maintained for each leaflet in the bacterial system. These bilayers were equilibrated for several hundred nanoseconds each before adding lipopeptides.

Before creating membrane simulations, we first built large water boxes with randomly distributed C16-KGG**K** lipopeptides. This system was run for several hundred nanoseconds, during which time the lipopeptides rapidly aggregated into micelles. A single large micelle was chosen arbitrarily and extracted. We removed enough lipopeptides to reduce the number to 48, which allowed us to easily make systems with a 10:1 lipid to lipopeptide ratio.

For each bilayer, we created 4 unique systems by manually placing the 48 lipopeptide micelle using VMD [28] such that the centroid of the micelle was between 60 and 80 Å from the centroid of the bilayer. We then added neutralizing sodium and chloride ions, with an excess to bring the concentration of free salt ions to approximately 100 mM.

To probe electrostatic selectivity, we created two more systems with the positive charges on the lysines removed, effectively rendering the peptides polar but chargeless. These systems are identical in composition to the POPE/POPG systems, with the exception of a minor change in the number of ions to maintain a system with a net zero charge.

All systems contained about 37,000 particles, including about 24,000 water beads, equivalent to about 300,000 total true atoms.

2.2. Simulation protocol

Our simulations were run using versions 4.0.5 and 4.5.4 of the GROMACS package [29,30]. We employed a time step of 10 fs as suggested by Winger et al., for accurate integration [31,32]. Furthermore, the neighbor list was updated every 5 steps. We held the temperature at 300 K using Nose-Hoover temperature coupling [33,34]. The pressure was treated semi-isotropically using the Parrinello–Rahman barostat [35], with a reference of 1 bar. Electrostatics were accounted for using a shift function with a coulomb cutoff of 12 Å. Shift was used for Van der Waals as well, with a switch distance of 9 Å and a cutoff of 12 Å.

We ran each simulation to an actual simulation time of at least 3 μs, though some trajectories were as long as 5 μs. Our total simulation time for this work, over all 10 systems, is about 46 μs. This can be thought of as an effective time of about 184 μs when we consider the suggested increase in kinetics due to the reduction of "friction" in our systems [27]. All the times we report here are actual simulation times. Snapshots were saved every 100 ps and it is at this resolution that all analysis was performed.

2.3. Simulation analysis

All analysis was done using tools developed with the Lightweight Object Oriented Structure library (LOOS) [36]. LOOS is an object-oriented structure library implemented in C++ and Boost, which provides a powerful library for creating new tools for the analysis of molecular dynamics simulations. LOOS is available for download at http://loos.sourceforge.net.

2.3.1. Fractional contacts analysis

To assess the chemical composition of the environment immediately surrounding the lipopeptides, we used fractional contact analysis. Specifically, we counted the number of beads of lipid species and water within an 8 Å radius. We then report a time series of the fraction of those particles that were water, lipids and other lipopeptides. We ignored ions

in this calculation, as they make up very few of the total number of atoms in the system.

2.3.2. Lipid density map

To measure the local enrichment of particular lipid species in the plane of the membrane, we generated a lipid density map. Specifically, for each frame we determined the centroid of each POPG molecule and created a 2D histogram using 1 $Å^2$ bins, normalizing to produce density in lipids/$Å^2$.

2.3.3. Radial distribution function

We computed the 2D radial distribution function (RDF) of various lipid species relative to lipopeptides in the membrane plane using the LOOS xy_rdf tool [37]. Each molecule was treated as a single point, located at its centroid. We also tracked the evolution of the RDF over time, breaking the trajectory into 10 ns windows.

2.3.4. Angle distribution

To assess the lateral ordering of lipid headgroups, we looked at the distribution of angles between sets of three POPG lipid headgroups (atom GL0, type P_4 in the MARTINI model). For each frame of the simulation, the angle was computed for each combination of 3 atoms where the distance between the end atoms and the center atom was shorter than 8 Å.

3. Results

3.1. Selectivity for POPE/POPG bilayers

Choosing to simulate models for both bacterial and mammalian bilayers allowed us to investigate the selectivity of C16-KGG**K** for bacterial systems. Fig. 2 shows the distance between the centroids of the AMLP micelle and the lipid bilayer, projected along the membrane normal. Part A shows the time series for each of the POPE/POPG ("bacterial") simulations. In each case, the micelle binds to the surface of the membrane (distance of 35 Å) within the first few hundred nanoseconds. At this point, the micelle remains intact, with a well-formed hydrophobic core; we will henceforth refer to this as the "bound" state.

In one of the four POPE/POPG simulations, the micelle actually inserts into the bilayer; this is seen in Fig. 2A as the curve that drops
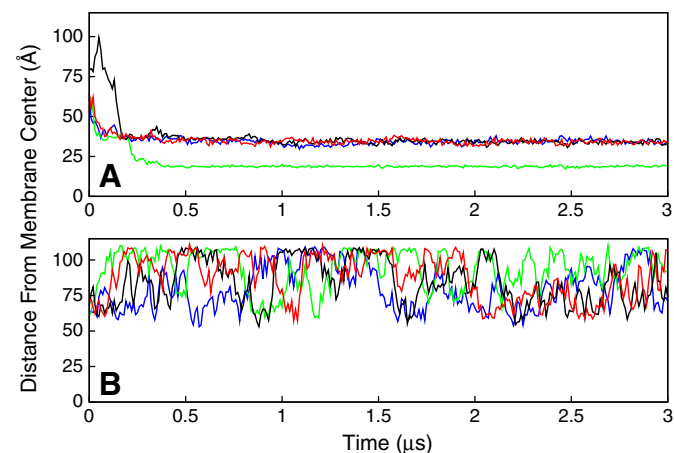
Fig. 2. Distance, in Å, between the centroids of the lipopeptide micelle and the lipid bilayer along the membrane normal as a function of time for both (A) POPE/POPG and (B) POPC. The apparent plateau around 110 Å for the POPC systems reflects the limitations of the periodic box (i.e. when the micelle wraps around the box, it begins to approach the bilayer from the other side). Four trajectories were run for each bilayer system.

below the bound state, with the final distance of 20 Å. After insertion, the micelle rapidly dissolves and the AMLPs disperse throughout the membrane, likely driven by AMLP–AMLP electrostatic repulsion. Fig. 3 shows images of this process.

By contrast, Fig. 2B shows that in the POPC ("mammalian") systems, the micelle does not approach—let alone bind—the membrane surface. The two simulations with a POPE/POPG bilayer and neutral lysines displayed a pattern identical to that for the POPC systems (data not shown). This makes intuitive sense, confirming that electrostatics are the primary driving force for AMLP-lipid binding. On the timescales simulated, the POPC bilayer is essentially invisible to the cationic micelle. For the POPE/POPG system, the net negative charge for the bilayer draws the micelle to the bound state only when the lipopeptides are cationic.

3.2. Preferential binding to POPG lipids

Considering the intermolecular contacts during the process of C16-KGG**K** micelle binding can provide insight into a mechanism for interaction and selectivity. Fig. 4 highlights the evolution of these intermolecular contacts as a function of time as the AMLPs bind and insert into the membrane. The micelle begins completely surrounded by water; inter-AMLP contacts are not shown, but are at their greatest early in the trajectory when the lipopeptides are in the micelle. As the micelle approaches the membrane, water contacts are replaced by contacts to lipids. A two-step process of lipid contact is clearly visible, with the first step, around 100 ns, showing association with the bilayer and progression to the bound state. In the second step, at ~200 ns, complete insertion occurs and there is a drastic increase in contact with lipids in the bilayer.

The significantly higher proportion of lipopeptides contacting POPG lipids, rather than POPE lipids, is particularly noteworthy. The difference is striking: in later portions of the trajectory, on average 40% of the contacts are to POPG, while about 25% are to POPE. This happens despite the fact that the relative proportion of POPE lipids in the bilayer is twice that of POPG. This demonstrates C16-KGG**K**'s strong affinity for POPG lipids.

3.3. Micelle binding locally enriches POPG

Fig. 5 shows POPG density for one trajectory, after the micelle has bound (but not inserted). In this bound state, POPG lipids are recruited to the space directly beneath the micelle, forming a small patch of nearly pure POPG. When we compare the two leaflets, reorganization is clearly limited to the leaflet to which the lipopeptides bound (Part A) and not the distal leaflet (Part B).

This effect can be further quantified through the use of a radial distribution function (RDF) in the plane of the bilayer, as seen in Fig. 6. Here we show the probability density of POPG lipids, POPE lipids and the complete bilayer as a function of distance from lipopeptides. Again, we only consider time in the trajectory after binding. The curve for all lipids is nearly a straight line at 1, indicating that the headgroups are not induced to pack more tightly near the micelle binding site. However, the POPG curve indicates an enrichment of POPG lipids at distances less than 40 Å, while the POPE density is diminished; this is precisely what would be expected if the POPG were preferentially attracted to the AMLPs, locally displacing the POPE. The tail end of each curve shows the opposite trend, with an enrichment of POPE lipids at long distances. We do not believe this is due to repulsion between the POPE and the AMLPs, but rather simply due to the limited box size, as the POPE lipids displaced at short distances are pushed to the outer edges of the box. In ideal conditions, with a significantly larger box, both the POPE and POPG curves would decay to 1 to represent bulk concentrations.

The lateral reorganization of the bilayer becomes more evident when we consider the time dependence of the RDF between POPG and
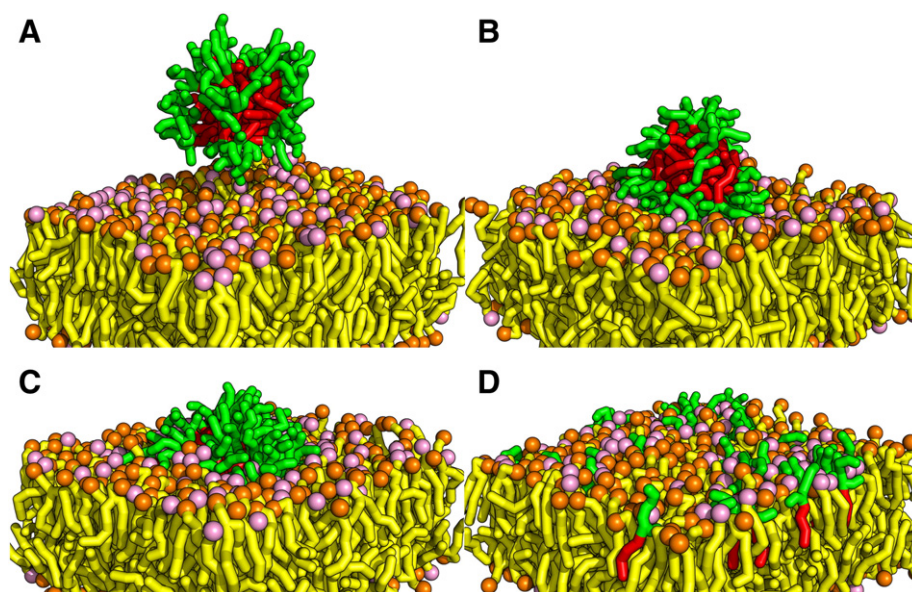
Fig. 3. Snapshots from the POPE/POPG binding simulation. Highlighted are the (A) initial structure; (B) bilayer binding at 120 ns; (C) insertion at 220 ns; (D) and lateral dispersion at 490 ns. The micelle is colored green and red, for the peptide and fatty acid tail, respectively. Lipid tails are colored yellow, while headgroups are colored pink and orange, for POPG and POPE, respectively.

the lipopeptides. Fig. 7 shows how the short-ranged enrichment of POPG evolves over time, both in the simulations where the micelle inserts (Part A) and in another where it merely remains bound to the membrane surface (Part B). Part A shows that the bilayer rapidly reorganizes as the micelle binds to the bilayer surface (the period roughly 100–200 ns into the trajectory), as POPG is recruited to the region under the micelle. Shortly after 200 ns insertion occurs, the POPG RDF drops dramatically, likely due to the dissipation of the lipopeptide micelle and the lateral dispersion of lipopeptides across the bilayer surface.

For the bound simulation, on the other hand, the recruitment of POPG lipids to the micelle continues throughout the trajectory. After about 600 ns, the maximum limit of aggregation appears to have been reached, and changes in the RDF are likely due to local fluctuations.

4. Discussion and conclusions

4.1. Mechanism of AMLP selectivity

In this work, the aim was to take advantage of the drastic speed increases available through coarse-grained molecular dynamics to characterize a potent antimicrobial lipopeptide, C16-KGG**K**. We ran a
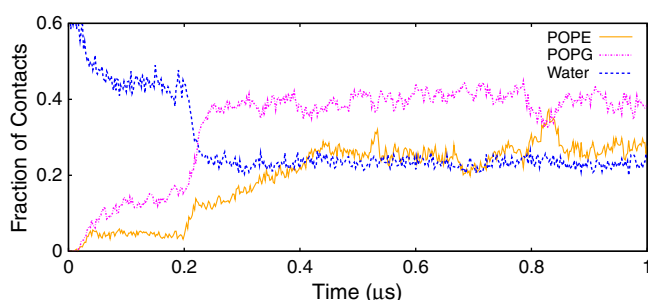
Fig. 4. Time series for the intermolecular contacts with C16-KGG**K**. Shows the POPE/POPG trajectory with complete lipopeptide insertion into the bilayer. The initial binding event occurs at about 120 ns, and insertion occurs at 200 ns. The missing remainder in total contacts are the inter-AMLP contacts.

number of simulations to demonstrate the selectivity of C16-KGG**K** for bacteria-like model bilayers to begin to characterize the specific mechanism by which the molecule may inhibit bacterial growth.

One intuitive hypothesis, based on the simple physical properties of the molecule, is that electrostatics are the driving force for selectivity for the bilayer. Our simulations are in agreement with this hypothesis, as micelles of C16-KGG**K** showed rapid association with the bilayer in the systems with model 2:1 POPE:POPG bilayers. However, if the electrostatic attraction is removed, either by using neutral POPC lipids or artificially neutralizing the lysines, binding is abolished. We built these systems to be as similar in composition as possible, with the exception of the lipid composition and minor differences in the number of ions used for system charge neutralization. With all of this in mind, electrostatics are the most likely cause of selectivity, drawing the lipopeptides to the bacterial bilayer prior to antibacterial activity.

4.2. Bilayer effects

While understanding selectivity may be fairly straightforward, probing the mechanism of action for C16-KGG**K** is not trivial. The processes of binding to the bilayer and eventual insertion are complicated, with many degrees of freedom and multiple factors. Our analysis of simulations with the bacteria-like bilayers has elucidated some key features in the binding process that may provide clues to a possible mechanism of action.

One of the most striking features of the simulations are the distinction between the bound and inserted states. Of the four binding systems, only one actually fully inserted. After complete micelle insertion, the lipopeptides, likely due to electrostatic repulsion, spread laterally across the bilayer in the leaflet on which binding occurred. At high concentrations of lipopeptides, this is probably the method of antibacterial activity, as interactions between the lipopeptides would drive insertion and lateral dispersion, leading to detergent-like permeabilization of the bilayer.

However, at lower concentrations, such as the micromolar concentrations at which these lipopeptides are able to inhibit microbial growth, this bilayer permeabilization is unlikely to be the primary mode of action. Our simulations suggest an alternative mechanism of action, based on the relatively "stable" bound state seen in the other three
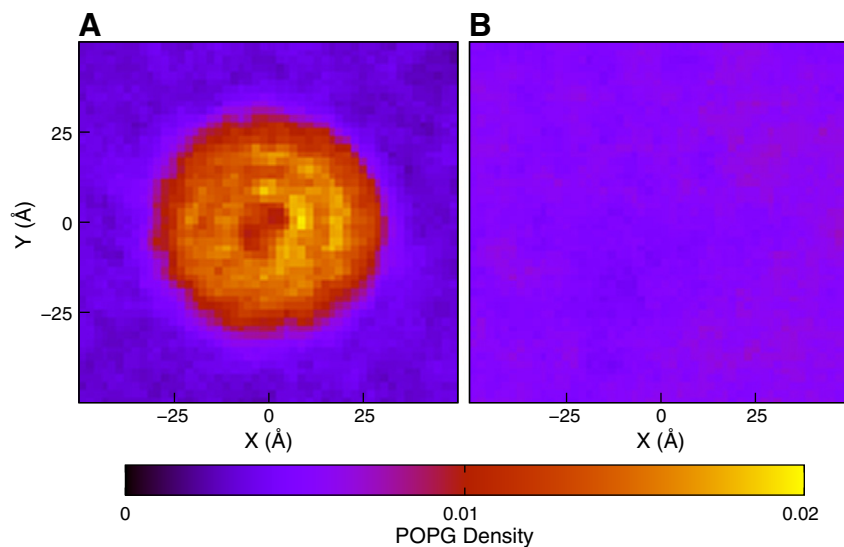
Fig. 5. Density of POPG lipids under the bound micelle, centered at the origin, for both the bound leaflet (A) and the unbound leaflet (B).

simulations. In this state, a raft-like region of highly ordered POPG lipids beneath the micelle provides stability and affords the micelle an extended period of time to further rearrange the bilayer (see Section 4.3 below). Based on a small number of trajectories, it appears that insertion either occurs very quickly (soon after binding, before the full formation of the pure POPG phase under the micelle), or very slowly (longer than the microsecond timescale of the simulations).

4.3. Bilayer crystallization

As discussed above, the presence of the lipopeptide micelle in the bound state causes drastic reorganization of the lipid bilayer. This reorganization leads to a high local concentration of POPG lipids in the region of the bilayer directly below the micelle. Upon visual inspection of this nearly pure patch of POPG bilayer, it appears that the bilayer may be crystallizing, with the formation of a small raft with high order and packing. Fig. 8 highlights this effect.

After roughly 500 ns in the bound state, the patch of bilayer beneath the micelle is composed entirely of POPG lipids (Part A). These lipids show ordered packing, with POPG headgroups aligned neatly into rows (Part B). This packing appears to be mediated by a similarly ordered interaction with the peptide portion of the lipopeptides (Part C); the

peptides curl around the phosphate, allowing both charged lysine chains to rest between a pair of neighboring lipid phosphates.

We demonstrate the shift in structural organization as a result of micelle binding by showing the distribution of angles formed by sets of 3 headgroups from POPG lipids for the bound state in one trajectory (Part D). The curves corresponding to the neat bilayer (free of lipopeptides) and the distal leaflet in bound simulations are nearly identical. Most sets of POPG headgroups form angles within two main regions, around 60 °C and 90 °C. The distributions are broad and diffuse, indicating variability in positioning between headgroup beads.

The third curve, corresponding to the leaflet in the bound simulation to which the lipopeptide micelle binds, shows a very different distribution. The primary modes are now positioned around 90 °C and nearly 180 °C, as expected in a rectangular lattice. The peaks are very narrow compared to the other curves, demonstrating that a large number of triplet sets are forming these 90 °C and 180 °C angles. This confirms our visual hypothesis that the POPG lipids form an ordered rectangular lattice when the lipopeptide micelle is present.
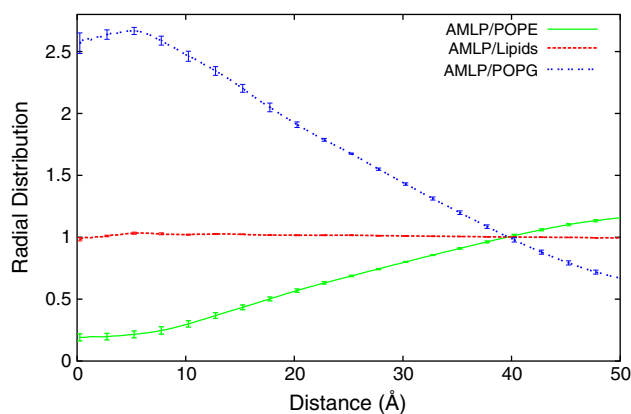
Fig. 6. Atomic density of POPE, POPG and all lipids as a function of distance from lipopeptides. Shown is the average of the bound state portions of the three trajectories that never inserted (with standard deviations for the three simulations).
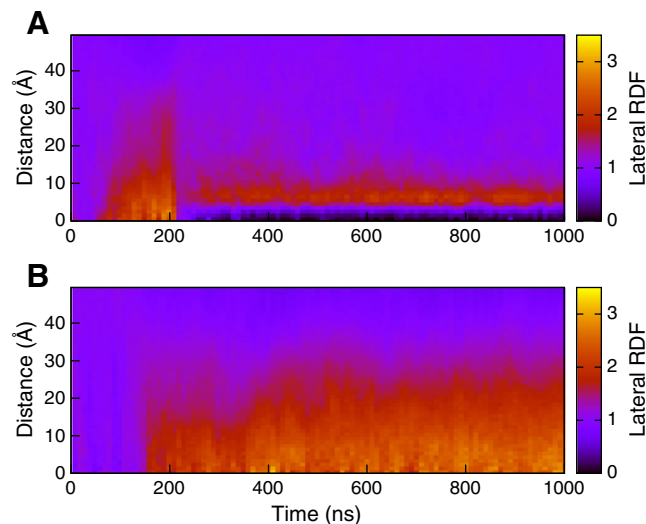
Fig. 7. Lateral radial distribution function for POPG lipids as a function of distance from lipopeptides plotted over time with 10 ns windows. Shown are (A) a simulation with lipopeptide insertion and (B) a simulation that remains in the bound state throughout the simulation.
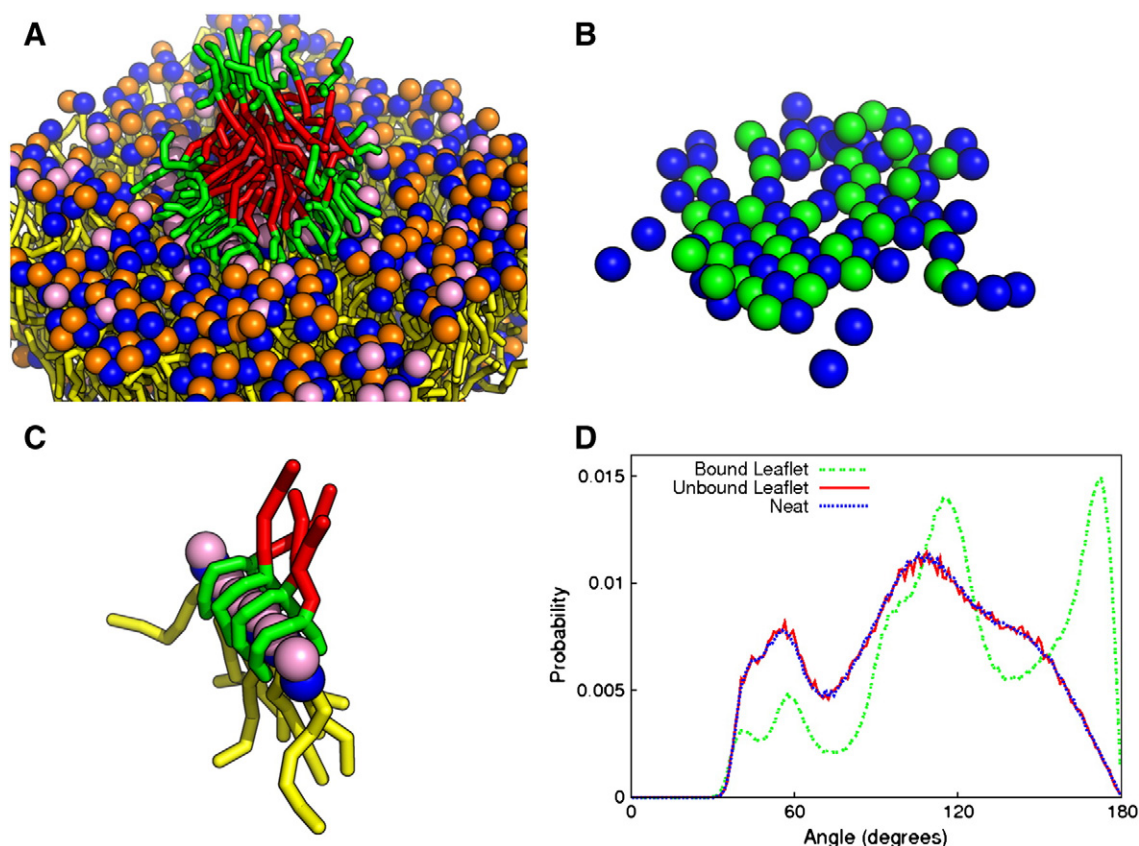
Fig. 8. Crystallization effects as a result of micelle binding. (A) Micelle bound to the bilayer (peptides in green, AMLP tails in red, POPG headgroups in pink, POPE headgroups in orange, and POPE/POPG phosphate groups in blue). (B) Visualization of headgroup "crystallization" under the micelle; POPG phosphates are blue and lipopeptide lysine amines are green. (C) Example of a row of POPG lipids maintained by interactions with C16-KGG**K** peptide. (D) Distribution of angles between triplets of POPG headgroups shorter than 8 Å apart.

Although we expected to see some ordering due to favorable peptide–lipid interactions, the degree of crystallization seems problematic. We suspect that this reflects a flaw in the force field. In contrast to an all-atom force field, where each particle has a partial charge, the only charged moieties in these systems are the lipid phosphates, POPE's NH_4, the lysine amines, and the free salt ions; water, which would ordinarily make strong polar interactions with these moieties, has zero charge in the MARTINI model. This, combined with the fact that MARTINI water is roughly four times larger than a water molecule, enhances the favorability of desolvating the lipid headgroups to create a lattice of oppositely charged phosphates and amines. Artifacts have been seen previously in simulations of charged peptides binding to bilayers using this model [38], suggesting that this may be a universal problem. For this reason, we plan to explore using the recently developed polarizable MARTINI water model in future work [39]. Coarse-grained models with higher-resolution electrostatics models are also very intriguing [40,41].

4.4. A possible mechanism of action

Recent work by many groups has described changes in bilayer reorganization and the localization of anionic lipids in response to the binding of cationic antimicrobial agents [42,43]. These results, combined with the present simulations, suggest a number of possible modes of action for AMPs and AMLPs. First, the presence of POPE and POPG rich domains could destabilize the bilayer, either by rapidly creating boundary defects between domains or by causing local changes in bilayer tension and curvature due to the tendency of lipids with PE headgroups to promote high negative curvature [44]. One could imagine anionic clusters also having an effect on membrane polarization,

possibly resulting in slow cell leakage [45,46]. Alternatively, the presence of bound AMLPs could alter the behavior of previously formed functional lipid domains. Membrane proteins that require certain local distributions of lipids may be impacted, as would proteins that are positioned along domain boundaries, which would be drastically redrawn [47]. Also, cellular processes that require large-scale reorganization of specific lipids, such as cell division, would be impacted.

A scaffold for successful bilayer phase separation by an antimicrobial agent has been suggested by Epand and Epand [48]. In their model, the molecule requires multiple cationic residues, significant hydrophobicity, and conformational flexibility. For C16-KGG**K**, these requirements are met, but micellization is likely an important part of the mechanism of action.

Given its structure, C16-KGG**K** is unlikely to exist as a monomer in solution except at very low concentrations; forming a micelle allows it to shield the hydrophobic acyl chain from water. Micelles also provide some level of stability necessary for C16-KGG**K** to bind to the bilayer surface and reorganize the bilayer without being immediately driven to insertion. Lastly, it allows C16-KGG**K** to cluster, creating a large structure of positive charge that, when bound to the surface, can create a large region of demixed POPG. Small clusters of the AMLP, or even individual molecules, if they were able to bind without inserting, would not be able to cause demixing at this level. Experimental work has shown that similar peptides are capable of forming macrostructures, including tubules and micelles [49].

4.5. Future work and conclusions

The present results suggest a number of avenues for future exploration. For example, it would be interesting to explore the

differences in binding affinity and bound conformation between a lipopeptide such as C16-KGG**K**, which is potent but not very selective, other related lipopeptides that are selective (e.g. C16-KA**A**K), and bacteria-inert lipopeptides (e.g. C16-KL**L**K) . Given the structural similarity of these lipopeptides—in the MARTINI model, they are nearly identical—it seems likely that a higher-resolution approach would be required, such as all-atom modeling. It would also be interesting to try to elucidate the transition state of micelle binding and insertion using a combination of umbrella sampling and commitor analysis [50].

The simplicity of our chosen systems implies another avenue for future work. For instance, major constituents to the systems of interest, such as cholesterol in mammalian bilayers, were omitted to maintain similarity to bilayers commonly used by experimental labs [18]. Exploring the effects of other components of the bilayer and other ratios of POPE to POPG in bacterial systems to reflect the known diversity in bilayers would provide significant insights into the relative selectivity and potency of C16-KGG**K**.

We are optimistic that understanding the biophysical properties of these novel antimicrobial lipopeptides and their mechanism of action at micromolar concentrations is critical to developing more potent and selective AMP and AMLP based antibiotics.

Acknowledgments

References

[1] H.G. Boman, Peptide antibiotics and their role in innate immunity, Annu. Rev. Immunol. 13 (1995) 61–92.

[2] H.G. Boman, H. Steiner, Humoral immunity in *Cecropia pupae*, Curr. Top. Microbiol. Immunol. 94–95 (1981) 75–91.

[3] M. Zasloff, Magainins, a class of antimicrobial peptides from xenopus skin: isolation, characterization of two active forms, and partial cDNA sequence of a precursor, Proc. Natl. Acad. Sci. U. S. A. 84 (1987) 5449–5453.

[4] H.V. Westerhoff, D. Juretić, R.W. Hendler, M. Zasloff, Magainins and the disruption of membrane-linked free-energy transduction, Proc. Natl. Acad. Sci. U. S. A. 86 (1989) 6597–6601.

[5] P.H. Mygind, R.L. Fischer, K.M. Schnorr, M.T. Hansen, C.P. Sönksen, S. Ludvigsen, D. Raventós, S. Buskov, B. Christensen, L.D. Maria, O. Taboureau, D. Yaver, S.G. Elvig-Jørgensen, M.V. Sørensen, B.E. Christensen, S. Kjaerulff, N. Frimodt-Moller, R.I. Lehrer, M. Zasloff, H.-H. Kristensen, Plectasin is a peptide antibiotic with therapeutic potential from a saprophytic fungus, Nature 437 (2005) 975–980.

[6] Z. Wang, G. Wang, APD: the antimicrobial peptide database, Nucleic Acids Res. 32 (2004) D590–D592.

[7] G. Wang, X. Li, Z. Wang, APD2: the updated antimicrobial peptide database and its application in peptide design, Nucleic Acids Res. 37 (2009) D933–D937.

[8] R.M. Epand, H.J. Vogel, Diversity of antimicrobial peptides and their mechanism of action, Biochim. Biophys. Acta 1462 (1999) 11–28.

[9] A.R. Koczulla, R. Bals, Antimicrobial peptides: current status and therapeutic potential, Drugs 63 (2003) 389–406.

[10] M. Zasloff, Antimicrobial peptides of multicellular organisms, Nature 415 (2002) 389–395.

[11] H. Jenssen, P. Hamill, R.E.W. Hancock, Peptide antimicrobial agents, Clin. Microbiol. Rev. 19 (2006) 491–511.

[12] K.A. Brogden, Antimicrobial peptides: pore formers or metabolic inhibitors in bacteria? Nat. Rev. Micro. 3 (2005) 238–250.

[13] B. Bechinger, K. Lohner, Detergent-like actions of linear amphipathic cationic antimicrobial peptides, Biochimica et Biophysica Acta (BBA)Biomembranes 1758 (2006) 1529–1539.

[14] Y. Shai, Z. Oren, From "carpet" mechanism to de-novo designed diastereomeric cell-selective antimicrobial peptides, Peptides 22 (2001) 1629–1641.

[15] R.E.W. Hancock, H.-G. Sahl, Antimicrobial and host-defense peptides as new anti-infective therapeutic strategies, Nat. Biotechnol. 24 (2006) 1551–1557.

[16] D. Avrahami, Y. Shai, Bestowing antifungal and antibacterial activities by lipophilic acid conjugation to D, L-amino acid-containing antimicrobial peptides: a plausible mode of action, Biochemistry 42 (2003) 14946–14956.

[17] D. Avrahami, Y. Shai, A new group of antifungal and antibacterial lipopeptides derived from non-membrane active peptides conjugated to palmitic acid, J. Biol. Chem. 279 (2004) 12277–12285.

[18] A. Makovitzki, D. Avrahami, Y. Shai, Ultrashort antibacterial and antifungal lipopeptides, Proc. Natl. Acad. Sci. U. S. A. 103 (2006) 15997–16002.

[19] A. Makovitzki, A. Viterbo, Y. Brotman, I. Chet, Y. Shai, Inhibition of fungal and bacterial plant pathogens in vitro and in planta with ultrashort cationic lipopeptides, Appl. Environ. Microbiol. 73 (2007) 6629–6636.

[20] H. Heller, M. Schaefer, K. Schulten, Molecular dynamics simulation of a bilayer of 200 lipids in the gel and in the liquid–crystal phases, J. Phys. Chem. 97 (1993) 8343–8360.

[21] R.W. Pastor, S.E. Feller, Time scales of lipid dynamics and molecular dynamics, in: K.M. Merz Jr., B. Roux (Eds.), Biological Membranes: A Molecular Perspective from Computation and Experiment, Birkhauser, 1996, pp. 3–30.

[22] E. Lindahl, M.S. Sansom, Membrane proteins: molecular dynamics simulations, Curr. Opin. Struct. Biol. 18 (2008) 425–431.

[23] E. Mátyus, C. Kandt, D.P. Tieleman, Computer simulation of antimicrobial peptides, Curr. Med. Chem. 14 (2007) 2789–2798.

[24] A.J. Rzepiela, D. Sengupta, N. Goga, S.J. Marrink, Membrane poration by antimicrobial peptides combining atomistic and coarse-grained descriptions, Faraday Discuss 144 (2010) 431–443 discussion 445–81.

[25] M. Louhivuori, H.J. Risselada, E. van der Giessen, S.J. Marrink, Release of content through mechano-sensitive gates in pressurized liposomes, Proc. Natl. Acad. Sci. U. S. A. 107 (2010) 19856–19860.

[26] J.H. Risselada, A.E. Mark, S.J. Marrink, Application of mean field boundary potentials in simulations of lipid vesicles, J. Phys. Chem. B 112 (2008) 7438–7447.

[27] S.J. Marrink, H.J. Risselada, S. Yefimov, D.P. Tieleman, A.H. de Vries, The MARTINI force field: coarse grained model for biomolecular simulations, J. Phys. Chem. B 111 (2007) 7812–7824.

[28] W. Humphrey, A. Dalke, K. Schulten, VMD: visual molecular dynamics, J. Mol. Graph. 14 (1996) 33–38 27–8.

[29] D. van der Spoel, E. Lindahl, B. Hess, G. Groenhof, A.E. Mark, H.J.C. Berendsen, GROMACS: fast, flexible, and free, J. Comput. Chem. 26 (2005) 1701–1718.

[30] B. Hess, C. Kutzner, D. van der Spoel, E. Lindahl, GROMACS 4: algorithms for highly efficient, load-balanced, and scalable molecular simulation, J. Chem. Theory Comput. 4 (2008) 435–447.

[31] M. Winger, D. Trzesniak, R. Baron, W.F. van Gunsteren, On using a too large integration time step in molecular dynamics simulations of coarse-grained molecular models, Phys. Chem. Chem. Phys. 11 (2009) 1934–1941.

[32] S.J. Marrink, X. Periole, D.P. Tieleman, A.H. de Vries, Comment on "on using a too large integration time step in molecular dynamics simulations of coarse-grained molecular models" by M. Winger, D. Trzesniak, R. Baron and W. F. van Gunsteren, Phys. Chem. Chem. Phys., 2009, 11, 1934, Phys. Chem. Chem. Phys. 12 (2010) 2254–2256 author reply 2257–8.

[33] S. Nose, M.L. Klein, Constant pressure molecular dynamics for molecular systems, Mol. Phys. 50 (1983) 1055–1076.

[34] W.G. Hoover, Canonical dynamics: equilibrium phase-space distributions, Phys. Rev. A 31 (1985) 1695–1697.

[35] M. Parrinello, A. Rahman, Polymorphic transitions in single crystals: a new molecular dynamics method, J. Appl. Phys. 52 (1981) 7182–7190.

[36] T.D. Romo, A. Grossfield, LOOS: an extensible platform for the structural analysis of simulations, Conf. Proc. IEEE Eng. Med. Biol. Soc. 2009 (2009) 2332–2335.

[37] T.D. Romo, A. Grossfield, LOOS: A lightweight object-oriented software library, 2010 http://loos.sourceforge.net.

[38] I. Vorobyov, L. Li, T.W. Allen, Assessing atomistic and coarse-grained force fields for protein–lipid interactions: the formidable challenge of an ionizable side chain in a membrane, J. Phys. Chem. B 112 (2008) 9588–9602.

[39] S.O. Yesylevskyy, L.V. Schäfer, D. Sengupta, S.J. Marrink, Polarizable water model for the coarse-grained MARTINI force field, PLoS Comput. Biol. 6 (2010) e1000810.

[40] P.A. Golubkov, P. Ren, Generalized coarse-grained model based on point multiple and Gay–Berne potentials, J. Chem. Phys. 125 (2006) 64103.

[41] P.A. Golubkov, J.C. Wu, P. Ren, A transferable coarse-grained model for hydrogen-bonding liquids, Phys. Chem. Chem. Phys. 10 (2008) 2050–2057.

[42] F. Jean-François, S. Castano, B. Desbat, B. Odaert, M. Roux, M.-H. Metz-Boutigue, E. J. Dufourc, Aggregation of cateslytin beta-sheets on negatively charged lipids promotes rigid membrane domains. a new mode of action for antimicrobial peptides? Biochemistry 47 (2008) 6394–6402.

[43] R.F. Epand, L. Maloy, A. Ramamoorthy, R.M. Epand, Amphipathic helical cationic antimicrobial peptides promote rapid formation of crystalline states in the presence of phosphatidylglycerol: lipid clustering in anionic membranes, Biophys. J. 98 (2010) 2564–2573.

[44] A. Arouri, M. Dathe, A. Blume, Peptide induced demixing in PG/PE lipid mixtures: a mechanism for the specificity of antimicrobial peptides towards bacterial membranes? Biochim. Biophys. Acta 1788 (2009) 650–659.

[45] I.S. Radzishevsky, S. Rotem, D. Bourdetsky, S. Navon-Venezia, Y. Carmeli, A. Mor, Improved antimicrobial peptides based on acyl-lysine oligomers, Nat. Biotechnol. 25 (2007) 657–659.

[46] S. Rotem, I.S. Radzishevsky, D. Bourdetsky, S. Navon-Venezia, Y. Carmeli, A. Mor, Analogous oligo-acyl-lysines with distinct antibacterial mechanisms, FASEB J. 22 (2008) 2652–2661.

[47] R.M. Epand, R.F. Epand, Bacterial membrane lipids in the action of antimicrobial agents, J. Pept. Sci. 17 (2011) 298–305.

[48] R.M. Epand, R.F. Epand, Lipid domains in bacterial membranes and the action of antimicrobial agents, Biochim. Biophys. Acta 1788 (2009) 289–294.

[49] A. Makovitzki, J. Baram, Y. Shai, Antimicrobial lipopolypeptides composed of palmitoyl di- and tricationic peptides, In vitro and in vivo activities, self-assembly to nanostructures, and a plausible mode of action, Biochemistry 47 (2008) 10630–10636.

[50] P.M. Kasson, E. Lindahl, V.S. Pande, Atomic-resolution simulations predict a transition state for vesicle fusion defined by contact of a few lipid tails, PLoS Comput. Biol. 6 (2010) e1000829.